SPIE Paper Number: 8358-43
SPIE Defense, Security, and Sensing
23-27 April 2012
Baltimore, Maryland, USA

Femtosecond fiber-laser-based laser-induced breakdown spectroscopy

Huan Huang*, Lih-Mei Yang and Jian Liu
PolarOnyx, Inc., 2526 Qume Drive, Suite 17 & 18, San Jose, CA, 95131, USA.

ABSTRACT

This paper reports the LIBS studies on elemental composition detection and identification by employing a femtosecond (fs) fiber laser. High quality LIBS spectra were obtained in air using near-infrared fs fiber laser coupled with a broadband high sensitivity spectrometer without gating control. Specific ion and neutral emission lines of different materials have been characterized by line scanning, including metals, glasses and even explosive materials. Different laser parameters including pulse energy, repetition rate, scanning speed and integration times have been investigated to optimize the sensitivity. Results show that faster scanning speed and higher pulse energies can greatly enhance the signal level and reduce the integration time. The LIBS spectra are highly reproducible at different repetition rates up to 1 MHz. Furthermore, detection of explosive materials was also achieved and both the constituent elemental emission and the CN and C_2 molecules emission were collected. Compared with conventional LIBS, fs fiber laser based LIBS system have advantages of less sample heating and damage, better spatial resolution and signal to background ratio, compact, reliable and cost-effective. This shows a potential portable LIBS system for versatile and rapid analysis of chemical and special explosive materials.

Keywords: Femtosecond laser, fiber laser, LIBS, explosive material, compact.

1. INTRODUCTION

Laser-Induced Breakdown Spectroscopy (LIBS) is a type of atomic emission spectroscopy that involves focusing a pulsed laser beam to generate plasma and excite a sample on the target surface, which can initially be in solid, liquid, or gaseous form. As a versatile and attractive analytical method, LIBS has the primary advantages of versatile sampling, rapid analysis, little or no sample preparation, sensitive to a wide variety of elements, simultaneous analysis of multi-elements, and small amounts of material and practically non-destructive. LIBS has been applied to the analysis of a number of materials including metals [1-3], semiconductors [4], bacterial samples [5-6], gases [7-8] and explosives [9-11]. The laser sources typically used is traditional solid state Nd:YAG lasers with nanosecond (ns) pulse duration and pulse energy of above 10 mJ level. For these lasers, a significant amount of the later part of the energy pulse goes into heating the plasma formed during the earlier part of the pulse through linear absorption. The plasma formed is very highly ionized which results in large amounts of continuum emission, especially at short time scales. Method of using of gated detector to reduce background emission and thus, improve the signal to noise ratio and minimize spectral interferences between species are needed. Another disadvantage of LIBS processes with long pulsed ns laser is large heat-affected zone as a result of linear absorption of the laser energy.

For femtosecond (fs) lasers, lower energies is needed for ablation compared with ns pulses due to shorter pulse duration, and less damage to surrounding materials and less ablation of material being analyzed by the laser spark occurs. Since ns laser pulses are not conducive to submicron spatial resolution owing to the imparted thermal diffusion length, use of fs laser is beneficial for improving spatial resolution and providing sufficient momentum for collision dominated breakdown process, and therefore improved LIBS signal to background emission ratio [1, 5-6, 12-13]. Therefore, fs lasers provide a LIBS process with lower ablation thresholds, improved sensibility, signal to background emission ratio and spatial resolution.

Meanwhile, to increase the sensitivity and limit of detection, much effort have been devoted to other approaches, such as sequential-pulse (or dual-pulse) LIBS including both the ns-ns and fs-ns combinations. And it has been demonstrated that the use of sequential-pulse (or dual-pulse) excitation can provide significant emission intensity enhancement relative to single pulse LIBS for different materials, thus providing lower limits of detection and allowing a wider range of

*hhuang@polaronyx.com; phone: 1 408 573-0934; fax 1 408 573-0932;

to be detected [4, 14-16]. Careful optimization of the double-pulse timing and temporal gating could lead to significant improvements in the double-pulse to single-pulse response ratio.

In this paper, a LIBS system based on fs fiber laser was used to study the elemental composition with non-intensified detector and without gating and delay. High quality LIBS spectra were obtained using near-infrared (1030 nm) fs fiber laser coupled with a high sensitivity detector. Emission lines of different materials have been characterized by surface line scanning, including metals, metal alloys and glasses. Different laser parameters including pulse energy, repetition rate and scanning speed have been investigated to study the influence to the LIBS signal. Furthermore, detection for explosive material - TNT on aluminum foil was also demonstrated using this technique. Not only the optical emission from the constituent elements of the explosive (C, H, N, and O) were identified, but also CN and C_2 molecules emission were observed as the marker for the explosive materials.

2. METHODS & MATERIALS

2.1 Experimental setup

The LIBS experimental setup used in this experiment is shown in Fig. 1. The fs laser system is a commercialized mode-locked seed fiber laser (PolarOnyx, Inc. - Uranus Series), generating 750 fs pulses (FWHM) at 1030 nm wavelength with pulse repetition rate tunable between 1 Hz and 1 MHz with an acousto-optic modulator (AOM). The output collimated beam is a nearly symmetric Gaussian with $M^2<1.3$ and the maximum output pulse energy is 10 μJ. The laser beam is focused into the sample by a microscope objective. The focal spot size for the laser beam can be calculated by $1.22\times\lambda / N.A.$, where λ is the laser wavelength and N.A. is the numerical aperture of the objective lens. Two focusing objectives are alternatively used - 50x (N.A. = 0.55) and 20x (N.A. = 0.4). Both of the focal spot diameters are less than 5 μm. An attenuator is used to control the laser pulse energy and a mechanical shutter is synchronized with the laser system. The total beam delivery loss is less than 20 percent. A CCD camera is used to obtain a live view for the laser direct writing. The sample is mounted on a motorized 3-D translation stage and the motion stage is controlled by computer to achieve different sample moving speeds. The dichroic mirror in the beam delivery system allows viewing of the target via a camera.

2.2 Materials

In this study, different bulk metals (Aluminum, Titanium, Stainless Steel and Copper), metal alloys (Brass and Invar) and glass materials (soda lime glass and fused silica) were used. The bulk targets of these materials are more than 0.5 mm thick and the surfaces were cleaned before the experiments. Samples with flat surfaces were chosen to allow for simple focusing onto a planar surface.

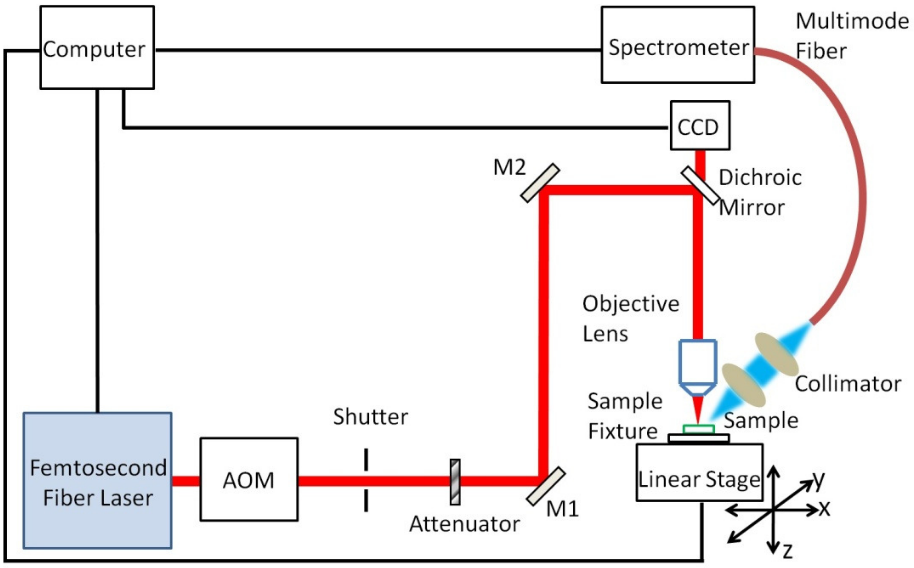

Figure 1. Femtosecond fiber laser induced breakdown spectroscopy experimental setup.

Samples of explosive material (2, 4, 6-trinitrotoluene or TNT) for LIBS were prepared by depositing solutions of explosives onto aluminum foils and allowing the solvent to evaporate. Solutions of TNT in acetone (50 mg/ml) were obtained from AccuStandard, Inc. The TNT that remained on the substrate after the evaporation of the solvent was melted and recrystallized to form a uniform layer on the substrate.

During the experiments, the target samples were translated in the transverse direction (Y axis) with the motion stage and the translation speed is from 0.1 mm/s to 100 mm/s. After each line translation, a step of increase will be added for X axis so that fresh sample surface will be ablated for LIBS signal collection. Pulse overlap may appear for each ablation spot along the scanning path depending on the scanning speed and repetition rate used. No quantification was attempted for this experiment.

2.3 LIBS signal collection

The optical emission from the plasma is collected by a collimator lens, coupled into a multimode optical fiber, and delivered to a spectrometer. A scientific-grade spectrometer (QE65000, Ocean Optics, Inc.) with high sensitively non-intensified detector was used and the spectral range of the spectrometer is from UV to NIR (200 - 950 nm). The collection optics is oriented at about 30 degrees above the processing location. The TE-cooled detector provides increased resolution and greater selectivity of the spectral information. The spectrometer is operated with a resolution of 1.9 nm. An optional filter may or may not be used during the experiment to block the laser wavelength. No gating electronics or digital delay generator were used for the recorded spectrum. Since the number of photons detected in a single-shot spectrum is relatively low for fs excitation compared with conventional LIBS laser pulses, accumulation of single-shot spectra allows a more complete spectrum to form. In this study, each observation consisted of acquiring multiple shots spectra and accumulating those spectra along the scanning path for analysis. The integration time is properly selected to obtained high quality spectrums based on different laser parameters and plasma intensity level. All the experiments are conducted in air atmosphere.

3. RESULTS & DISCUSSION

3.1 Fundamental study

An important characteristic of emitting plasma induced by fs laser pulses is related to the absence of interactions between the laser beam and the formed expanding plasma. This effect provides background continuum lower than those induced by ns laser pulses, which can be considered as an advantage in order to obtain good analytical results even without gated detectors [6, 9, 17-18]. However the line intensity emissions are also lower to be detected and this can be seen as a drawback for the technique sensitivity. In this experiment, line scanning was used and the emitted plasmas by multiple pulses interactions was collected and averaged for the characteristic analysis to overcome this drawback. For each individual spectrum, a fresh surface of the sample was presented and scanned.

Along the scanning path, different pulse repetition rates and scanning speed were used, so laser pulses may be overlapped for each spot depending on the pulse repetition rate and the scanning speed. If there is no pulse overlap, the single pulse ablation fluence F can be defined by Eq. (1):

$$F = \frac{2E}{\pi \times (D/2)^2} \tag{1}$$

Where E is the single pulse energy, D is the focal spot diameter.

Figure 2 shows the emitted LIBS spectrum for metal block - Aluminum with pulse energy of 0.75 µJ and repetition rate 225 kHz. The sample scanning speed is 2 mm/s and the total integration time for spectrum collection is 0.5 s. So the trace in the figure represents the sums of single spectrum from 112,500 laser firings. But there is no pulse overlap for each ablation spot along the scanning path, the single pulse ablation fluence used is 22.7 J/cm^2. The two strongest peaks in the spectrum are Aluminum emission lines with wavelengths of 309.28 nm and 396.16 nm.

Figure 3 shows another representative emitted LIBS spectrum for soda lime glass surface ablation with pulse energy of 3.0 µJ and repetition rate 225 kHz. The scanning speed is 4 mm/s and the total integration time for spectrum collection is 0.5 s. So the trace represents the same number of summation of single laser spectrum as Fig. 2 and the single pulse ablation fluence used is 90.8 J/cm^2. The strong peaks in the spectrum are referring to Ca (393.36 nm & 396.85 nm), Mg (517.27 nm & 518.36 nm), Na (588.98 nm) and K (766.49 nm & 769.90 nm), respectively. For both Fig. 2 and Fig.3, one filter was added when collecting the LIBS signal to block the laser wavelength, so only visible range of the spectrum can be seen.

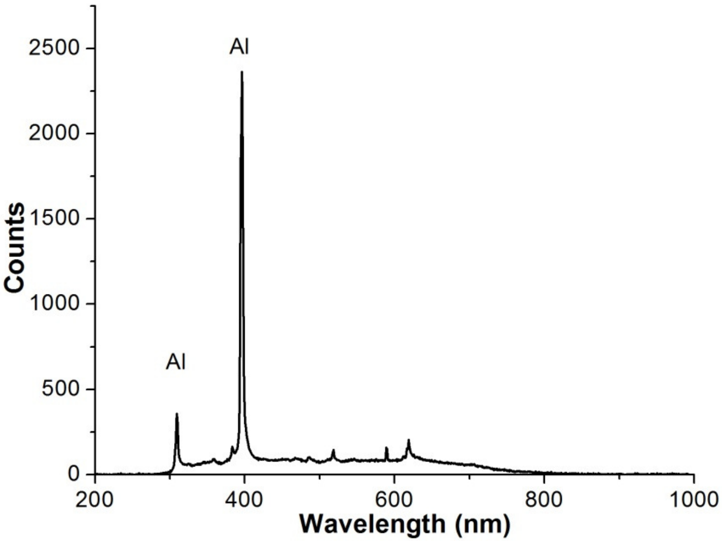

Figure 2. LIBS signal obtained from Aluminum block (0.75 µJ & 225 kHz, 2 mm/s scanning speed).

As shown in Fig.2 & 3, the spectra show some radiation continuum (smooth portion on the ground) with atomic lines above it. Although it is accumulated over many individual spectra, the plasma emission continuum is minimal in contrast to what is commonly observed with ns laser with higher pulse energies. This is consistent with other reported LIBS workers with ultra short pulsed lasers [2-3, 11]. This benefit of fs LIBS suggests that non-gated non-intensified spectral acquisition can be used for this LIBS application, which in turn means that high repetition rate laser ablation and long spectral integration time can be used without negative consequences on the quality of the spectra. Furthermore, this also can be applied in real time feedback and control for laser material processing by means of measuring optical emission spectrum generated during the processing.

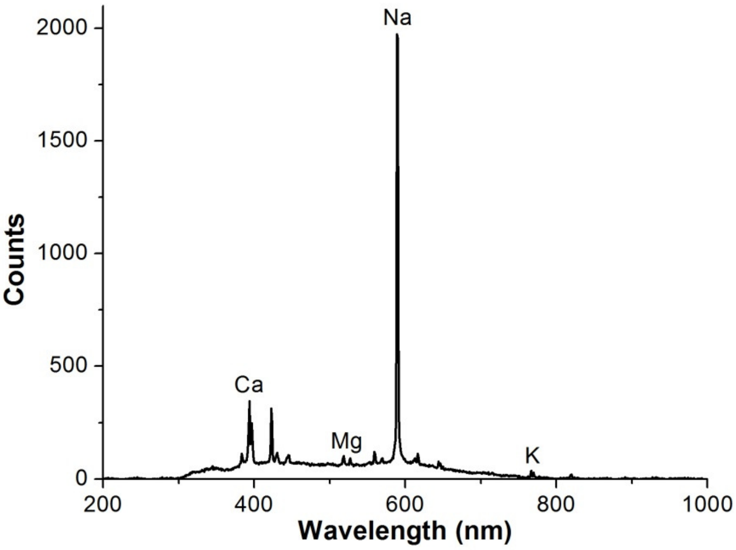

Figure 3. LIBS signal obtained from soda lime glass (3 µJ & 225 kHz, 4 mm/s scanning speed).

3.2 Influence of laser parameters

The LIBS measurements are sensitive to many variables, including laser parameters such as the wavelength, the pulse energy, the pulse duration, the scanning speed and the pulse-to-pulse power fluctuation, and other factors such as focusing condition and ambient conditions. Here different pulse energies and scanning speeds were investigated to study the influence of the LIBS signal.

Figure 4 shows the LIBS signal for Brass block with different pulse energies – 0.75 µJ, 1.50 µJ and 3.0 µJ from bottom to top, respectively. The other laser processing parameters include 225 kHz repetition rate and 0.1 mm/s scanning speed. The spectrometer integration time is 0.5 s. There is pulse overlap for each spot and the pulse overlap rate is 2.25 pulses/µm, which is defined by the repetition rate over the scanning speed. The strong peaks in the spectrums are identical and are referring to Cu (324.75 nm, 327.40 nm, 510.55 nm, 515.32 nm, 521.82 nm), and Zn (472.22 nm & 481.05 nm). As shown in Fig. 4(a), both the peaks and continuum signal levels are increasing with the increasing of the pulse energy for the same scanning speed and integration time. But the signal-to-background ratio does not change as shown in Fig. 4(b), which means both the atomic emission and the background continuum emission increase simultaneously with the increased pulse energy.

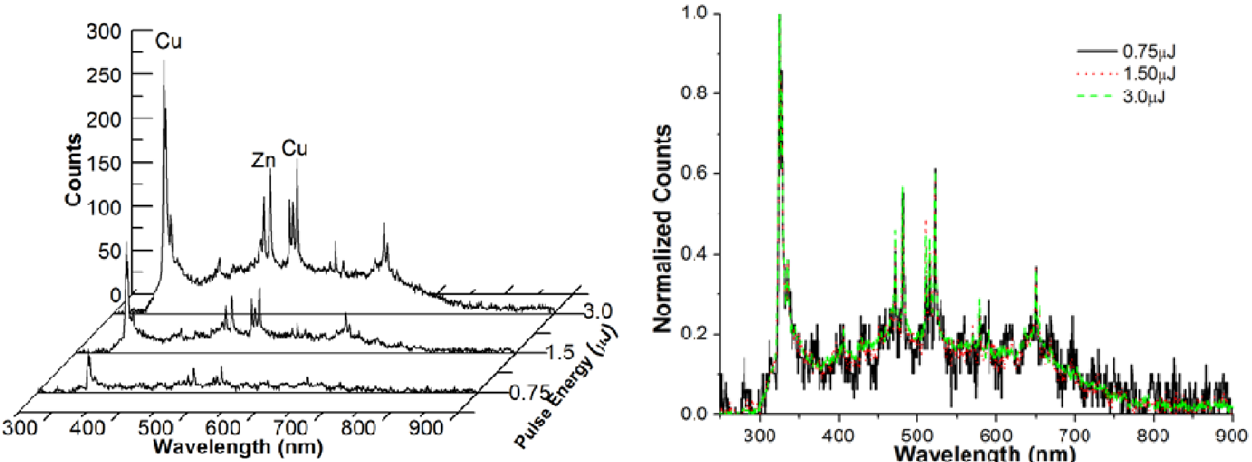

(a) (b)

Figure 4. LIBS signal obtained from Brass block with different pulse energies - 0.75, 1.5, 3.0 µJ from bottom to top: (a) real counts; (b) normalized counts.

Figure 5 shows the LIBS signal for Brass block with different scanning speeds - 0.1 mm/s, 0.2 mm/s, 0.4 mm/s, 1.0 mm/s, 2.0 mm/s, 4.0 mm/s, 10.0 mm/s and 20.0 mm/s from bottom to top, respectively. The other laser processing parameters are the same - 225 kHz repetition rate, 3.0 µJ pulse energy and 0.5 s integration time. The same trend is observed - both the peaks and continuum signal levels are increasing when the canning speed changes from 0.1 mm/s to 10 mm/s. The intensity level reaches the maximum at about 10 mm/s and the intensity is almost the same when the speed changes from 10 mm/s to 20 mm/s. Furthermore, the intensity level is decreasing when further increasing the scanning speed from 20 mm/s to even higher. The main reason for this change is that for slower scanning speeds, there is many pulse overlaps for each ablation spot especially for scanning speed less than 1.0 mm/s, so the overlapped pulse firings do not make much contribution to LIBS signal due to the focus position and the ablated material by previous pulses. When the scanning speed is higher, there is less or even no pulse overlap along the scanning path, so each pulse firing is incident to fresh material spot and this greatly increases both the atomic emission and background continuum emission. However, when the scanning speed is even higher, the ablation threshold will be increased due to less pulse overlap [19-20] and the LIBS signal intensity will become weaker.

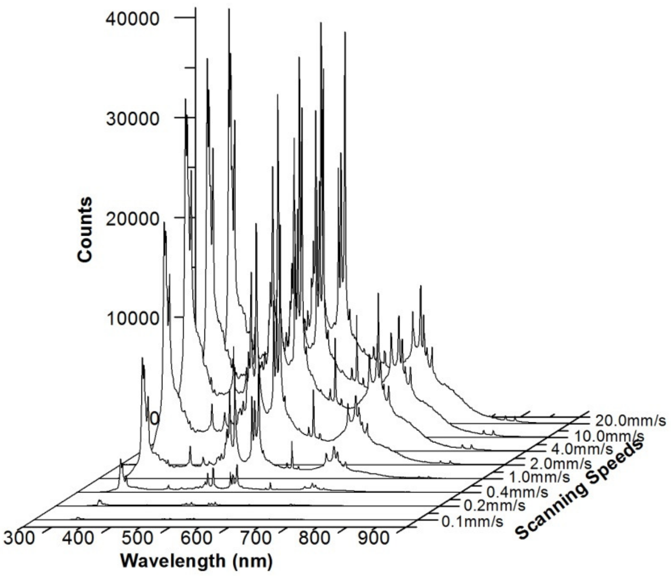

Figure 5. LIBS signal obtained from Brass block with different scanning speeds - 0.1 – 20.0 mm/s from bottom to top.

3.3 Explosive materials

Figure 6 shows the fs LIBS signal for TNT on Aluminum foil with line scanning. The pulse energy used is 3.0 µJ and repetition rate is 225 kHz. The scanning speed is 40 mm/s and the total integration time for spectrum collection is 2 s. A significant portion of the laser energy is absorbed by the aluminum foil due to the thin TNT residue thickness. The two strongest peaks in the spectrum are aluminum emission lines from the substrate with wavelengths of 309.28 nm and 396.16 nm (saturated). Emission from the elemental constituents of the explosive include: C (247.86 nm, not shown here due to filter block), H (656.56 nm), N (747.02 nm), and O (777.32 nm). The oxygen peak is a product of three closely spaced transitions of neutral oxygen at wavelengths of 777.19 nm, 777.42 nm, and 777.54 nm.

Moreover, molecular emission from CN (388.32 nm) and C_2 (516.54 nm) are observed as shown in the Fig.6, which are important representative peaks for explosive material LIBS signal. This spectral feature is the product of a sequence of electronic transitions from the second excited electronic level to the ground electronic level with no change in the vibrational quantum number [21]. This emission has also been observed in the previous studies on ns and fs LIBS of explosives [9-10, 12, 22].

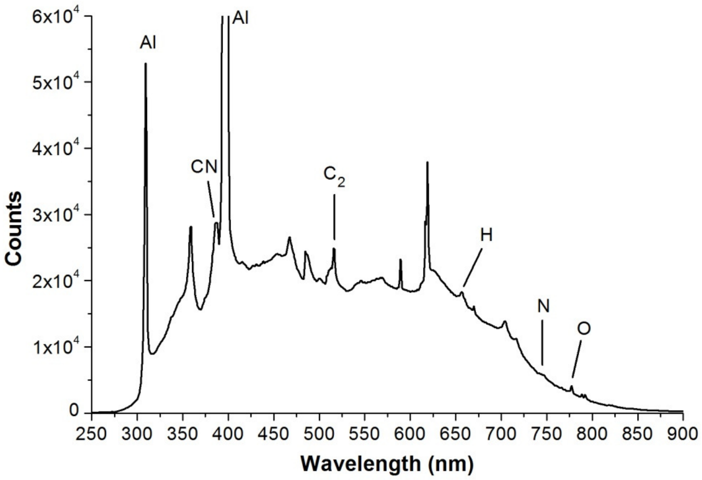

Figure 6. LIBS signal obtained from TNT on Aluminum foil (3 µJ, 225 kHz, 40.0 mm/s & 2 s integration time).

The LIBS plasma is a complex system that consists of interactions not only of the laser with the sample, but also the laser with the plasma and the plasmas with the atmosphere. This is particularly important issue when dealing with organic samples due to the fact that many of the elements that are selected as discriminators are also commonly found in air. For example, most explosive materials predominantly contain carbon, hydrogen, oxygen, and nitrogen. Atmospheric oxygen and nitrogen entrained in the plasma will contribute to the atomic emission from the oxygen and nitrogen from the explosive sample. In addition, if the substrate is an organic material the carbon and hydrogen will interfere with the atomic emission from the explosive.

However, it was pointed out that the LIBS plasma from fs regime has minimized interference and contributions from the atmosphere and the fs laser interaction is better than ns laser interaction to build a stable library for discrimination of organic compounds [6, 10, 23]. Any CN formation from carbon and nitrogen recombination that may occur is not visible above the noise in the air atmosphere for fs laser regime.

Thus, explosive material detection could be realized by using fs fiber laser with non-gated non-intensified detector and it has advantages such as less continuum background, less air entrainment, and less substrate interrogation. This is very beneficial for explosive residue detection from both cost analysis point of view and compact size point of view. This commercial fs laser system is more reliable and reasonably inexpensive compared with fs solid state lasers. No expensive components (ICCD & delay generator) are needed and compact fiber laser systems can be used instead of more costly bench top laser systems.

4. SUMMARY

Elemental composition detection and identification by utilizing fs fiber laser line scanning at atmospheric pressure have been demonstrated for LIBS applications. High quality LIBS spectra were obtained using relatively low-energy and the emission lines of different materials including metals, metal alloys and glasses have been characterized. Different laser parameters including repetition rate, scanning speed and pulse energies have been studied to enhance the signal level. Results show that faster scanning speed and higher pulse energies can greatly enhance the signal level and the obtained spectrum is highly reproducible at different repetition rates up to 1 MHz. Thus, real-time feedback and processing control for laser material processing is possible with the current technique especially for laser processing of materials, such as cutting, thin film scribing and thin layer removing or deposition.

Furthermore, the results shown also demonstrate that detection of explosive residues can be achieved by using fs LIBS with non-gated non-intensified detector. Both the constituent elemental emission (H, N, and O) and the CN and C_2 molecules emission were collected for the explosive materials. Advantages attributed to the fs fiber laser LIBS that could improve the detection of explosive residue include cost-effective, compact size, minimized background continuum and negligible atmospheric entrainment. This can lead to a more compact, reliable, low-cost and field-deployable detection system for versatile and rapid analysis of chemical and special explosive materials.

Future works with this fs fiber laser LIBS technique include the investigation of laser parameters to enhance the signal-to-background ratio and the further reduction of the continuum background.

ACKNOWLEDGE

This work was partially funded by NSF and Army SBIR programs.

REFERENCES

[1] Margetic, V., Pakulev, A., Stockhaus, A., Bolshov, M., Niemax, K., and Hergenröder, R., "A comparison of nanosecond and femtosecond laser-induced plasma spectroscopy of brass samples," Spectrochimica Acta Part B: Atomic Spectroscopy 55(11), 1771-1785 (2000).

[2] Hwang, D. J., Jeon, H., Grigoropoulos, C. P., Yoo, J., and Russo, R. E., "Femtosecond laser ablation induced plasma characteristics from submicron craters in thin metal film," Applied Physics Letters 91(25), 251118-251118-3 (2007).

[3] Le Drogoff, B., Margot, J., Chaker, M., Sabsabi, M., Barthelemy, O., Johnston, T., Laville, S., Vidal, F., and Von Kaenel, Y., "Temporal characterization of femtosecond laser pulses induced plasma for spectrochemical analysis of aluminum alloys," Spectrochimica Acta Part B: Atomic Spectroscopy 56(6), 987-1002 (2001).

[4] Amal, K., Elnaby, S., Palleschi, V., Salvetti, A., and Harith, M., "Comparison between single-and double-pulse LIBS at different air pressures on silicon target," Applied Physics B: Lasers and Optics 83(4), 651-657 (2006).

[5] Assion, A., Wollenhaupt, M., Haag, L., Mayorov, F., Sarpe-Tudoran, C., Winter, M., Kutschera, U., and Baumert, T., "Femtosecond laser-induced-breakdown spectrometry for Ca 2+ analysis of biological samples with high spatial resolution," Applied Physics B: Lasers and Optics 77(4), 391-397 (2003).

[6] Baudelet, M., Guyon, L., Yu, J., Wolf, J. P., Amodeo, T., Fréjafon, E., and Laloi, P., "Femtosecond time-resolved laser-induced breakdown spectroscopy for detection and identification of bacteria: A comparison to the nanosecond regime," Journal of Applied Physics 99, 084701 (2006).

[7] Tran, M., Smith, B. W., Hahn, D. W., and Winefordner, J. D., "Detection of gaseous and particulate fluorides by laser-induced breakdown spectroscopy," Applied Spectroscopy 55(11), 1455-1461 (2001).

[8] Ball, A., Hohreiter, V., and Hahn, D., "Hydrogen leak detection using laser-induced breakdown spectroscopy," Applied Spectroscopy 59(3), 348-353 (2005).

[9] Dikmelik, Y., McEnnis, C., and Spicer, J. B., "Femtosecond and nanosecond laser-induced breakdown spectroscopy of trinitrotoluene," Optics Express 16(8), 5332-5337 (2008).

[10] De Lucia, F. C., Gottfried, J. L., and Miziolek, A. W., "Evaluation of femtosecond laser-induced breakdown spectroscopy for explosive residue detection," Optics Express 17(2), 419-425 (2009).

[11] Leahy-Hoppa, M. R., Miragliotta, J., Osiander, R., Burnett, J., Dikmelik, Y., McEnnis, C., and Spicer, J. B., "Ultrafast Laser-Based Spectroscopy and Sensing: Applications in LIBS, CARS, and THz Spectroscopy," Sensors 10(5), 4342-4372 (2010).

[12] Sreedhar, S., Kumar, M. A., Kumar, G. M., Kiran, P. P., Tewari, S. P., and Rao, S. V., "Laser Induced Breakdown Spectroscopy of RDX and HMX with nanosecond, picosecond, and femtosecond pulses," Proc. of SPIE 7665, 76650T (2010).

[13] Le Drogoff, B., Chaker, M., Margot, J., Sabsabi, M., Barthélemy, O., Johnston, T., Laville, S., and Vidal, F., "Influence of the laser pulse duration on spectrochemical analysis of solids by laser-induced plasma spectroscopy," Applied Spectroscopy 58(1), 122-129 (2004).

[14] Lawrence-Snyder, M., Scaffidi, J., Angel, S. M., Michel, A. P. M., and Chave, A. D., "Sequential-pulse laser-induced breakdown spectroscopy of high-pressure bulk aqueous solutions," Applied Spectroscopy 61(2), 171-176 (2007).

[15] Asgill, M. E., Brown, M. S., Frische, K., Roquemore, W. M., and Hahn, D. W., "Double-pulse and single-pulse laser-induced breakdown spectroscopy for distinguishing between gaseous and particulate phase analytes," Applied optics 49(13), C110-C119 (2010).

[16] Windom, B., Diwakar, P., and Hahn, D., "Dual-pulse Laser Induced Breakdown Spectroscopy for analysis of gaseous and aerosol systems: Plasma-analyte interactions," Spectrochimica Acta Part B: Atomic Spectroscopy 61(7), 788-796 (2006).

[17] Eland, K. L., Stratis, D. N., Gold, D. M., Goode, S. R., and Angel, S. M., "Energy dependence of emission intensity and temperature in a LIBS plasma using femtosecond excitation," Applied Spectroscopy 55(3), 286-291 (2001).

[18] Eland, K. L., Stratis, D. N., Lai, T., Berg, M. A., Goode, S. R., and Angel, S. M., "Some comparisons of LIBS measurements using nanosecond and picosecond laser pulses," Applied Spectroscopy 55(3), 279-285 (2001).

[19] Baudach, S., Bonse, J., and Kautek, W., "Ablation experiments on polyimide with femtosecond laser pulses," Applied Physics A: Materials Science & Processing 69(7), 395-398 (1999).

[20] Huang, H. and Guo, Z., "Ultra-short pulsed laser PDMS thin-layer separation and micro-fabrication," Journal of Micromechanics and Microengineering 19, 055007 (2009).

[21] Lurie, J. B. and El-Sayed, M., "Chemiluminescence of cyano radicals formed from reaction of nitric oxide with multiphoton electronic excitation photofragments of toluene," The Journal of Physical Chemistry 84(25), 3348-3351 (1980).

[22] De Lucia, F. C., Gottfried, J. L., Munson, C. A., and Miziolek, A. W., "Multivariate analysis of standoff laser-induced breakdown spectroscopy spectra for classification of explosive-containing residues," Applied optics 47(31), G112-G121 (2008).

[23] Brown, C., Baudelet, M., Bridge, C., Fisher, M., Sigman, M., Dagdigian, P., and Richardson, M., "Atmosphere issues in detection of explosives and organic residues," Proc. SPIE 7304, 73041D (2009).